

LINE SHIFTS, BROAD-LINE REGION INFLOW, AND THE FEEDING OF ACTIVE GALACTIC NUCLEI

C. MARTIN GASKELL^{1,2} AND RENÉ W. GOOSMANN^{3,4,5,6}

¹ Department of Astronomy, University of Texas, Austin, TX 78712-0259, USA; martin.gaskell.astro@gmail.com

² Centro de Astrofísica de Valparaíso y Departamento de Física y Astronomía, Universidad de Valparaíso, Av. Gran Bretaña 1111, Valparaíso, Chile

³ Astronomical Institute of the Academy of Sciences, Bocni II 1401, 14131 Prague, Czech Republic; rene.goosmann@astro.unistra.fr

⁴ Observatoire Astronomique de Strasbourg, Université de Strasbourg, CNRS, UMR 7550, 11 rue de l'Université, 67000 Strasbourg, France

Received 2008 May 27; accepted 2013 March 25; published 2013 May 2

ABSTRACT

Velocity-resolved reverberation mapping suggests that the broad-line regions (BLRs) of active galactic nuclei (AGNs) can have significant net inflow. We use the *STOKES* radiative transfer code to show that electron and Rayleigh scattering off the BLR and torus naturally explains the blueshifted profiles of high-ionization lines and the ionization dependence of the blueshifts. This result is insensitive to the geometry of the scattering region. If correct, then this model resolves the long-standing conflict between the absence of outflow implied by velocity-resolved reverberation mapping and the need for outflow if the blueshifting is the result of obscuration. The accretion rate implied by the inflow is sufficient to power the AGN. We suggest that the BLR is part of the outer accretion disk and that similar magnetohydrodynamic processes are operating. In the scattering model, the blueshifting is proportional to the accretion rate so high-accretion-rate AGNs will show greater high-ionization line blueshifts, as is observed. Scattering can lead to systematically too high black hole mass estimates from the C IV line. We note many similarities between narrow-line region (NLR) and BLR blueshiftings, and suggest that NLR blueshiftings have a similar explanation. Our model explains the higher blueshifts of broad absorption line QSOs if they are more highly inclined. Rayleigh scattering from the BLR and torus could be more important in the UV than electron scattering for predominantly neutral material around AGNs. The importance of Rayleigh scattering versus electron scattering can be assessed by comparing line profiles at different wavelengths arising from the same emission-line region.

Key words: accretion, accretion disks – black hole physics – galaxies: active – line: profiles – quasars: emission lines – scattering

Online-only material: color figures

1. INTRODUCTION

The structure and kinematics of the broad-line region (BLR) of thermal active galactic nuclei⁷ (AGNs) has long been a subject of much debate, and a wide range of structures and velocities have been considered (for reviews see Mathews & Capriotti 1985; Osterbrock & Mathews 1986; Osterbrock 1993; Gaskell et al. 1999; Sulentic et al. 2000; Gaskell 2009). Because of these uncertainties, for a long time it was not clear where the BLR is located, what it is doing, and hence what role it plays in the AGN phenomenon. Reverberation mapping (Lyutyi & Cherepashchuk 1972; Cherepashchuk & Lyutyi 1973; Blandford & McKee 1982; Gaskell & Sparke 1986) has enabled us to probe the structures of the BLR and dusty torus, and it is argued elsewhere (see Gaskell et al. 2007, hereinafter “GKN”; and Gaskell 2009) that the BLR and torus share a similar flattened toroidal structure with a high covering factor and self-shielding.

A major reason for the uncertainty over the structure and kinematics of the BLR has been the conflicting pictures of the velocity field in AGNs field given by varying lines of observational evidence. First, the discovery of broad absorption lines (Lynds 1967) was unequivocal evidence that at least *some* gas is outflowing from AGNs. Radiatively driven outflows could also naturally explain the symmetric “logarithmic” BLR

line profiles seen in a large fraction of AGNs (Blumenthal & Mathews 1975). The outflow picture was supported by the discovery (Gaskell 1982) of the blueshifting of the high-ionization BLR lines with respect to the low-ionization lines and the rest frame of the host galaxy by ~ 600 km s⁻¹. This effect, which for brevity we will refer to here simply as “blueshifting,” required physical separation of the high- and low-ionization BLR clouds, a component of radial motions, and an opacity source. Gaskell (1982) proposed a “disk-wind” model where the blueshifting could be explained by having the high-ionization clouds be radially outflowing, with obscuration in the equatorial plane blocking our view of the receding clouds (i.e., of the redshifted side of the line profile). Although the blueshifting is usually of the order of ~ 600 km s⁻¹, it can exceed 4000 km s⁻¹ (Corbin 1990). The blueshifting is not only found when comparing the profiles of high- and low-ionization lines in individual AGNs, but also when using spectral principal component analysis (SPCA) of samples of AGNs to separate out line profiles into possible independent components such as an “intermediate-line region” (ILR) and a “very broad line region” (VBLR; see Brotherton et al. 1994). The magnitude of the blueshifting is roughly in order of increasing ionization potential (Tytler & Fan 1992). It also tends to be strongest in luminous, radio-quiet AGNs (Corbin 1990; Tytler & Fan 1992; Sulentic et al. 1995; Richards et al. 2002), especially in broad absorption line QSOs (BALQSOs; Corbin 1990; Richards et al. 2002), and in AGNs with a high accretion rate (Sulentic et al. 2000; Xu et al. 2003; Leighly & Moore 2004). The large blueshifts in high-accretion-rate AGNs have been taken as an indication of strong outflowing winds in these AGNs (e.g., Leighly & Moore 2004; Komossa et al. 2008).

⁵ Tinsley Visiting Scholar, Department of Astronomy, University of Texas, Austin, TX 78712-0259, USA.

⁶ Current address: Observatoire astronomique de Strasbourg, 11 rue de l'Université, F-67000 Strasbourg, France.

⁷ For a review of the differences between thermal and non-thermal AGNs, see Antonucci (2012).

Gaskell (1988) pointed out that the outflowing high-ionization BLR scenario predicted strong velocity-dependent time delays in the wings of the high-ionization lines (the blue wing should lead the red wing by twice the line-continuum delay), and showed that such a signature of outflowing winds was absent at a high confidence level in velocity-resolved reverberation mapping of NGC 4151. This has subsequently been found to be the case in many other AGNs where velocity-dependent time delays have been studied (Koratkar & Gaskell 1989, 1991a, 1991b; Crenshaw & Blackwell 1990; Korista et al. 1995; see Gaskell 2010b for more detailed discussion). With only a couple of exceptions discussed below, the wings of BLR lines either vary simultaneously (as would be expected from Keplerian motion of the clouds or isotropic motions), or show slight evidence for inflow (i.e., the red wings vary first). Because of the strong evidence for gravitational domination of the motions, Gaskell (1988) argued that motions of BLR clouds were gravitationally dominated, and hence that they could be used for determining black hole masses. Furthermore, Krolik et al. (1991) showed from an analysis of the Clavel et al. (1991) observations of NGC 5548 that broad-line widths are consistent with the $r^{-1/2}$ fall off with radius expected when motions are virialized. The Krolik et al. result has been confirmed for other objects (Peterson & Wandel 2000; Onken & Peterson 2002; Kollatschny 2003) covering a wide range of black hole masses and Eddington ratios.

There has thus long been little doubt that *low*-ionization BLR clouds (i.e., those producing Mg II and the Balmer lines) are predominantly orbiting the black hole. Other lines of evidence point to this orbital motion being Keplerian motion in the equatorial plane. Despite the significant covering factor of the BLR, we never see the BLR in absorption (see GKN), Balmer line widths show the expected correlation with the orientation of the rotation axis (Wills & Browne 1986; Rokaki et al. 2003), disk-like line profiles are common (e.g., Eracleous & Halpern 1994; Gaskell & Snedden 1999), and evidence of orbital motion of emission regions has been detected (Gaskell 1996; Sergeev et al. 2002; Pronik & Sergeev 2006). It has been suggested that double-peaked line profiles are due to separate BLRs around two supermassive black holes in a binary (Gaskell 1983) but variability observations strongly support a disk origin instead (see Gaskell 2010a and references therein). Gaskell (2010c, 2011) shows that apparently extreme double BLR peaks can readily be explained with the same gas distribution and kinematics as for single-peaked BLRs seen from a slightly higher inclination. The question of the detectability of close supermassive binary black holes remains an active area of investigation, however (see Popović 2012 for an extensive review).

It can be seen that there is considerable confidence that black hole masses can reliably be estimated from *low*-ionization lines (see Marziani & Sulentic 2012 for a review of AGN black hole mass determinations). However, for the *high*-ionization lines, the conflict between the kinematics implied by the blueshifted absorption lines and the blueshifting of the emission lines on the one hand, and the velocity-resolved reverberation mapping on the other, has raised serious doubts about the suitability of high-ionization lines such as C IV $\lambda 1549$ for estimating black hole masses. Further evidence for a difference in the kinematics of high- and low-ionization lines comes from the different velocity dependencies of the physical conditions (Snedden & Gaskell 2004). The ionizing flux received by low-ionization BLR lines shows the dependence on velocity one would expect as a result

of virialization and the inverse-square law, while the ionizing flux received by the high-ionization clouds appears to be almost independent of velocity.

This conflict between BLR kinematic indicators cannot simply be reconciled by assuming that the low-ionization lines arise in a disk while the high-ionization lines arise in a wind (e.g., Collin-Souffrin et al. 1988) because the velocity-resolved reverberation mapping specifically shows (Gaskell 1988; Koratkar & Gaskell 1989, 1991a; Crenshaw & Blackwell 1990) that the *high*-ionization BLR gas is *not* outflowing. Also, the $r^{-1/2}$ fall off of line widths with radius (Krolik et al. 1991) includes the high-ionization C IV line. Furthermore, disk-wind models have a problem of explaining why line profiles of different ions are so similar if they have very different origins (Tytler & Fan 1992). While winds necessarily exist in AGNs in order to remove angular momentum so that material can accrete, and they could be energetically important as well, the amount of mass involved is small. The density in a wind is more than an order of magnitude lower than in the disk, and emissivity goes as the square of the density, so emission from a wind is negligible.

In this paper, we will argue that the velocity-resolved reverberation mapping results are correct, and that the *entire* BLR has a net inflow. In Section 2, we summarize the evidence for an inward spiraling of the BLR and estimate the inflow component of velocity. In Section 3, we argue that scattering is consistent with producing a blueshifting when the BLR is inflowing, and in Section 4 we use the *STOKES* Monte Carlo radiative transfer code to show that scattering off an inflowing medium reproduces observed blueshifted line profiles and also explains the dependence of blueshifting on ionization. We consider the implications of the inflowing BLR scenario for the energy generation mechanism in AGNs in Section 5. In Section 6, we offer an explanation of why high-accretion-rate AGNs (“narrow-line Seyfert 1s” = NLS1s) show a stronger blueshifting, we point out potential systematic effects when the C IV emission line is used to estimate masses of high-redshift AGNs, we suggest an extension of our model to the narrow-line region (NLR), and we offer an explanation of why the blueshifting is enhanced in BALQSOs.

2. INFLOWING BLR GAS

2.1. The Evidence for an Inflow Velocity Component

Although it has generally been assumed in estimating black hole masses that the BLR gas is in near-Keplerian or quasi-random orbits (i.e., there is no net radial motion), Gaskell (1988) found that for NGC 4151 *inflow* was favored and that purely Keplerian or random orbits were excluded at the 97% (single-tailed) confidence level. Koratkar & Gaskell (1989) similarly found that non-inflowing motion was excluded in Fairall 9 at the $\sim 95\%$ confidence level. From the intensive 1989 *IUE* monitoring of NGC 5548 (Clavel et al. 1991), Crenshaw & Blackwell (1990) and Done & Krolik (1996) also favored a net inflow of the C IV emitting gas in NGC 5548. From the estimated errors in the lags given by Crenshaw & Blackwell (1990), non-inflowing motion is excluded at the 93% confidence level. The 1993 combined *Hubble Space Telescope* and *IUE* campaign (Korista et al. 1995) showed a similar degree of inflow (see their Table 25). The only bright AGN for which the variability of C IV has been studied is 3C 273, where Koratkar & Gaskell (1991b) and Paltani & Türler (2003) find an inflowing velocity component at two separate epochs. As Gaskell & Snedden (1997) point out, although the statistical significance

of inflow C IV for one line in any one observing campaign of any individual AGN is not necessarily strong, the case is much stronger when all the AGNs are considered together.⁸ The aforementioned analyses are mostly for C IV λ 1549, but Gaskell (1988) found inflow of Mg II λ 2798 in NGC 4151, and Welsh et al. (2007) have recently found that H β in NGC 5548 has an inflow component of velocity.

Two contradictory velocity-resolved reverberation mapping results must be mentioned. The first is an event in NGC 5548 which temporarily showed an apparent outflow kinematic signature (Kollatschny & Dietrich 1996). The second is a similar conflicting signature seen in one season of monitoring of NGC 3227 (Denney et al. 2009). The temporary NGC 5548 apparent outflow signature certainly does not represent a systematic outflow because only three months later an inflow signature was seen in the same object (Kollatschny & Dietrich 1996). Gaskell (2010c, 2011) has shown that transient apparent outflow signatures are a natural consequence of off-axis variability for which there is considerable other evidence.

Independent evidence for inflow comes from high-resolution spectropolarimetry (Smith et al. 2005). The systematic change in polarization as a function of velocity across the Balmer lines suggests a net inflow of a scattering region somewhat exterior to the Balmer lines.

In summary, we believe that there is significant observational evidence for gas producing both the high- and low-ionization BLR lines to be inflowing.

2.2. The Inflow Velocity

We can estimate the ratio of net inflow velocities to random velocities along the line of sight from the positions of the peaks of the red-wing/blue-wing cross correlation functions (CCFs). The positions of the expected peaks in the wing-wing CCFs are marked in Gaskell (1988) and Koratkar & Gaskell (1989). The observed peak positions and the one found by Crenshaw & Blackwell (1990) are all consistent with the net inflow velocities being several times smaller than the non-inflow velocities. Done & Krolik (1996) reach a similar conclusion from more detailed modeling of the velocity-dependent delays in NGC 5548. For each object this suggests that the net inflow velocity of C IV is $\sim 1000 \text{ km s}^{-1}$. In a totally independent analysis of the polarization structure of Balmer lines, Smith et al. (2005) suggest an inflow velocity of the scattering region of 900 km s^{-1} . We will therefore adopt an inflow velocity of 1000 km s^{-1} . However, we will see below that the precise value of the inflow velocity is not critical for our modeling and that the blueshifting can be obtained with much lower velocities.

3. PRODUCING A BLUESHIFT FROM INFLOWING GAS

There are two main ways of producing a blueshift of a line from inflowing gas. One is by having anisotropic emission from the gas clouds (Gaskell 1982; Wilkes 1984), and the other is by having scattering off inflowing material (e.g., Auer & van Blerkom 1972). Although the emission from BLR clouds is certainly expected to be anisotropic, the anisotropy is much greater for some lines than for others. As discussed by Wilkes & Carswell (1982) and Kallman et al. (1993), this creates a problem in explaining all line profiles with an inflowing anisotropic emitting cloud model. Ly α has particularly strongly

asymmetric emission compared with other lines when clouds are optically thick, which is almost certainly the case for the BLR clouds of relevance here (see Snedden & Gaskell 2007 for evidence against a significant optically thin contribution to the BLR). There is no evidence that Ly α is more asymmetric than other lines (Wilkes & Carswell 1982), so it would be hard for anisotropic emission from inflowing clouds to explain the blueshifting.

Electron scattering has long been considered to be a significant source of line broadening in AGNs in general (Kaneko & Ohtani 1968; Weymann 1970; Mathis 1970), and from time to time it has been invoked to explain the line profiles of individual objects (Shields & McKee 1981; Laor 2006).⁹ Scattering regions with a net radial motion were considered by Auer & van Blerkom (1972). If the scattering region is outflowing, then scattered photons are redshifted, while if it is inflowing, then photons are blueshifted. This can easily be understood by considering one's reflection in a moving mirror (see Figure 10 of Gaskell 2009). If the mirror is moving toward you, then your image appears to be approaching at twice the speed of the mirror. Such shifts have already been shown in simulations of electron scattering in AGNs by Kallman & Krolik (1986) and Ferrara & Pietrini (1993) and it has been suggested that this could be a cause of the blueshifting of high-ionization lines (Corbin 1990; Mathews 1993).

4. SCATTERING IN AN INFLOWING MEDIUM

4.1. Spherical Scattering Shells

We have modeled the effects of an inflowing scattering medium using the STOKES Monte Carlo radiative transfer code, which is described in Goosmann & Gaskell (2007) and Marin et al. (2012). Detailed documentation, sample input, source code, and executables for different computer platforms can be freely downloaded.¹⁰ The optical depths, τ_{es} , to scattering by free electrons along our line of sight are not expected to be much greater than unity inside the high-ionization BLR of an AGN. Shields & McKee (1981) estimate $\tau_{\text{es}} \lesssim 1$ for electrons between BLR clouds, and Laor (2006) estimates $\tau_{\text{es}} \approx 0.3$ for typical BLR clouds. Modeling of BLR clouds with the photoionization code CLOUDY (Ferland et al. 1998) gave similar values of τ_{es} . We therefore investigated quasi-spherical external scattering regions with $\tau = 0.5, 1, \text{ and } 2$. We also modeled $\tau = 10$ to investigate effects of significantly larger optical depths. The inflow velocity was taken to be 1000 km s^{-1} in all models. Since in this paper we are interested in modeling just the inflow and line asymmetry, we simply assumed that the unscattered line had an intrinsic broadening due to bulk motions. The assumed unbroadened profile is shown as a solid black line in Figure 1. We considered inflowing scattering shells both inside and outside the BLR. The results are shown in Figure 1.

Our first result is that for a line-emitting region outside an inflowing scattering shell there was a negligible effect on the line profile (differences mostly smaller than the plotting lines and symbols in the figures). This thus verifies that when there is strong radial stratification of the BLR (see GKN and Gaskell 2009), only the innermost high-ionization lines (those within the scattering region) are blueshifted. This gives a natural explanation of the difference in blueshift with ionization and is

⁸ Koratkar & Gaskell (1991b) also find non-statistically significant C IV inflow in four additional AGNs.

⁹ Note, however, that the apparent extended wings in the AGN considered by Shields & McKee (1981) are actually due to red continuum being too low in the Baldwin (1975) spectrum (J. M. Shuder 1981, private communication).

¹⁰ www.stokes-program.info

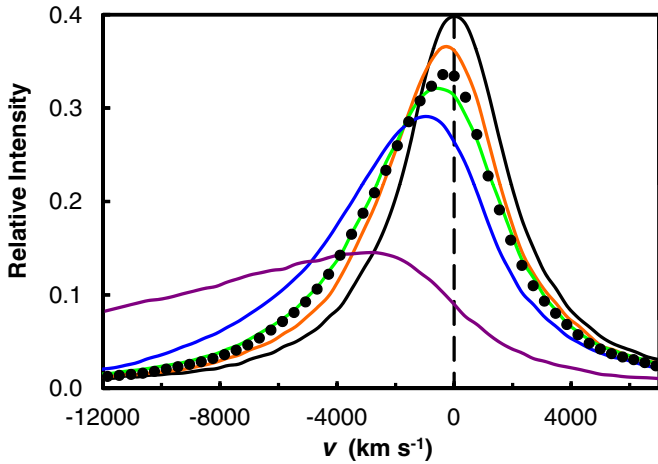


Figure 1. Calculated shifts of the C IV line by electron or Rayleigh scattering. The top black solid curve shows a Lorentzian line profile before scattering. The other solid curves show the blueshifting caused by an external spherical shell of scatterers with an inflow velocity of 1000 km s^{-1} . The areas under all curves are the same. In order of increasing blueshifting and decreasing peak flux, the curves show the effects of $\tau = 0.5$ (red), 1.0 (green), 2.0 (blue), and 10 (purple). The dots show the blueshifting caused by an inflowing flared disk with a radial optical depth of 5, a half-opening angle of 60° , and an inflow velocity of 1000 km s^{-1} , when the BLR is viewed from a “type 1” viewing position.

(A color version of this figure is available in the online journal.)

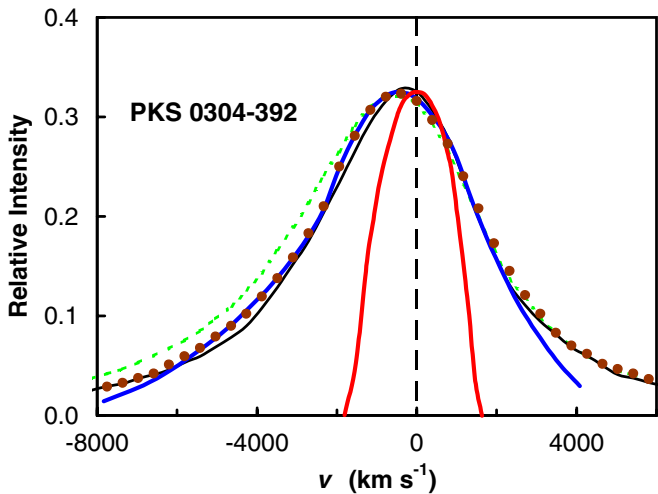


Figure 2. The profiles of O I $\lambda 1305$ (narrow symmetric profile shown in red) and C IV $\lambda 1549$ (thick blue line) for the quasar PKS 0304-392. The thin black line is the blueshifted profile produced by a spherical distribution of scatterers with $\tau = 0.5$, and the dashed green line is the profile produced by the same distribution with $\tau = 1$. The brown dots are the profile produced by a $\tau = 20$ inflowing cylindrical distribution. PKS 0304-392 observations taken from Wilkes (1984).

(A color version of this figure is available in the online journal.)

a big advantage of our scattering model over the outflowing-wind-plus-obscuration model of Gaskell (1982) because in the latter model one has to contrive to have the obscuration affect the outer low-ionization lines less. In our scattering model, the blueshift of a line only depends on the optical depth and velocity of material *outside* where the line is emitted. As discussed in Section 4.4 below, we can therefore easily predict blueshifting as a function of ionization. For example, C III] $\lambda 1909$ will have a blueshifting about half that of C IV $\lambda 1549$, as is observed to be the case (Corbin 1990; Steidel & Sargent 1991).

In Figure 2, we show a comparison with the blueshifted C IV profiles in a typical AGN, and in Figure 3 we show a comparison

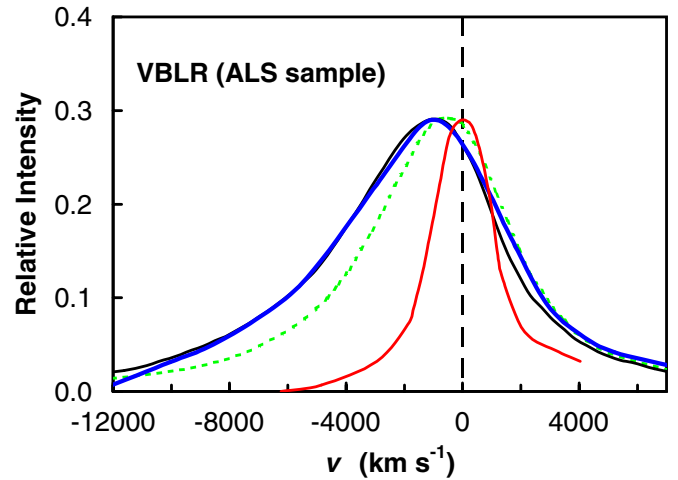


Figure 3. The mean intermediate line region (ILR) profiles (narrow red profile), and very broad line region (VBLR) profiles (thick blue line) given by SPCA of the ALS sample of Brotherton et al. (1994). The solid line shows the shifting caused by an external spherical shell of scatterers with $\tau = 2$ inflowing at 1000 km s^{-1} as shown in Figure 1. The dotted green line is for a similar shell with $\tau = 1$.

(A color version of this figure is available in the online journal.)

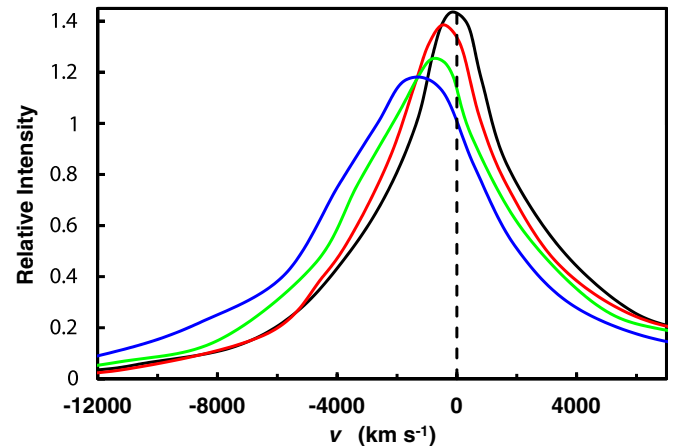


Figure 4. Shifts in composite SDSS spectra binned by C IV blueshift. Each curve is based on approximately 50 AGNs (see Richards et al. 2002 for details). The blueshifts of each sample are 197, 606, 1003, and 1526 km s^{-1} for the black, red, green, and blue curves, respectively. No attempt has been made to remove blending with He II $\lambda 1640$ or O III] $\lambda 1663$. To match Figure 1, the areas under all curves are the same—i.e., they have been normalized to the same combined flux in the C IV, He II, and O III] blend. These line profiles can be compared with the model predictions of Figure 1.

(A color version of this figure is available in the online journal.)

with the VBLR line profile given by SPCA of a sample of AGNs by Brotherton et al. (1994) in. In Figure 4, we show the blueshifts for composite SDSS spectra (Richards et al. 2002) sorted by blueshift.

It can be seen in Figure 1 that for a spherical shell, the blueshifting and asymmetry increase with τ . For $\tau \sim 10$ (a much greater electron-scattering optical depth than has been considered for the line of sight to a BLR), both the blueshifting and the asymmetry become much greater than is observed (see Figures 2–4), so we can rule out such high optical depths along the line of sight.

4.2. Rayleigh Scattering in the BLR and Torus

While large electron scattering optical depths are not likely along our line of sight to the BLR or within the inner BLR, our modeling of BLR clouds with *CLOUDY* showed that for clouds of sufficiently large neutral column densities to produce the significant Fe II emission seen in many AGNs, Rayleigh scattering was over an order of magnitude more important than electron scattering in the UV. This is not surprising for a region where hydrogen, which is the main provider of electrons, is mostly neutral, since a typical Rayleigh cross section is larger in the UV than the Thomson cross section. The potential importance of Rayleigh scattering in modifying the spectra of AGNs has been discussed in detail by Korista & Ferland (1998), and Lee (2005) has considered the effect of Rayleigh scattering on the polarization of Ly α .

STOKES does not explicitly handle Rayleigh scattering at present, but the angular dependence of Rayleigh scattering and electron scattering is identical, and the variation of scattering cross section across an emission line is unimportant, so Rayleigh scattering can be treated as electron scattering. The effect of Rayleigh scattering off an inflowing medium completely covering the source will be to give a very large blueshift as shown in Figure 1 for $\tau \sim 10$. Such Rayleigh scattering would, however, be accompanied by substantial blueshifted low-ionization absorption which is never observed. We can therefore strongly rule out such a *spherical* shell which is optically thick to Rayleigh scattering.

4.3. Scattering Off a Flattened BLR and Torus

Although it is unlikely that our direct line of sight to the BLR has a high optical depth to electron scattering, as one goes away from the black hole the BLR must become optically thick (in order to explain the strong optical Fe II emission) and merge with the torus (see GKN), so the optical depth to both electron and Rayleigh scattering will become substantial in the equatorial plane (Korista & Ferland 1998). The existence of Compton-reflection humps (Pounds et al. 1990) is evidence that there are substantial electron scattering optical depths. Reprocessing of X-rays requires $\tau_{\text{es}} > 1$ (see, e.g., Goosmann et al. 2007 for some modeling of reprocessed X-ray spectra emerging from AGN accretion disks). It is also well known that half of all Seyfert 2 galaxies are observed to be ‘‘Compton thick’’ (Risaliti et al. 1999), so most or all AGNs are probably optically thick to electron scattering in the equatorial plane. Gaskell et al. (2007) have argued that in a typical AGN, the BLR, like the torus, has a covering factor of 40% or so. As Smith et al. (2004) and Smith et al. (2005) point out, a significant scale height of the scattering region is also necessary in order to explain the polarization of type 1 AGNs. The broadband polarization properties as a function of opening angle are considered in detail in Marin et al. (2012). We therefore modeled an inflowing scattering cylindrical torus with a half-opening angle of 60° , an optical depth of 5, and an inflow velocity of 1000 km s^{-1} . The viewing position is within the half-opening angle (i.e., as required for a type 1 viewing position). We show the profiles arising from such a model by the dotted curve in Figure 1.

It can be seen from Figure 1 that the blueshifting produced by such a model differs insignificantly from that produced by the purely spherical scattering model with $\tau \sim 1$ or 2. However, unlike the spherical model, the shift produced in the torus model depends only on the inflow velocity, and except for small opening angles (where the flared disk begins to approximate a

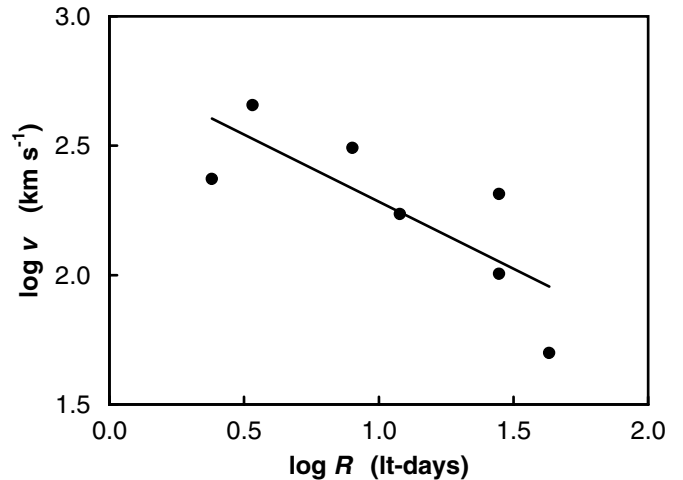


Figure 5. Mean blueshifts of emission lines (see text for details) vs. the radii, R , of maximum emission predicted in the GKN model. The line is a least-squares fit showing $\log v$ as a function of $\log R$.

shell) the shift is less sensitive to large optical depths. This is because in the torus case, after one or two scatterings a photon has a high probability of escape within the half-opening angle. The main difference between the quasi-spherical scattering case and the torus case is that the former produces more blueward asymmetry for a given inflow velocity and optical depths. For most objects, such as the AGN shown in Figure 2, the difference between the two models is negligible. The advantages of such a flattened BLR and torus are that there is no need to fine tune τ , and high Rayleigh scattering optical depths are permitted.

The precise geometry of the inflowing region is not important, only the covering factor. As an illustration of this the dots in Figure 2 show the profile resulting from scattering off an optically thick cylindrical inflow. This can again be seen to give a line profile similar to an inflowing shell of $\tau \sim 1$. The similarity of line profiles for a range of geometries is easy to understand because the observed profile is simply the sum of the unscattered profile plus a scattered blueshifted profile. The size of the scattered component depends on the covering factor, and its shift depends on the inflow velocity and the number of scatterings.

Note that in all our models there is some degeneracy between inflow velocity and covering factor, and, if the covering factor is large, with the optical depth as well (see Figures 1 and 2). This means that our adopted v_{inflow} of 1000 km s^{-1} is not critical. If $v_{\text{inflow}} < 1000 \text{ km s}^{-1}$, then the observed blueshifts can readily be reproduced by increasing the covering factor and/or τ of the scattering medium. For example, a scattering region with a half-opening angle of 60° , $v_{\text{inflow}} = 700 \text{ km s}^{-1}$, and $\tau_{\text{scatt}} = 1$ gives essentially identical profiles as $v_{\text{inflow}} = 100 \text{ km s}^{-1}$ and $\tau_{\text{scatt}} = 10$. On the other hand, it is not likely that $v_{\text{inflow}} > 1000 \text{ km s}^{-1}$ or else the blueshifting predicted will exceed the observed shifts.

4.4. Blueshifting as a Function of Emission Radius

Our scattering model predicts that the blueshift of a line depends on the inflow velocity immediately outside the radius, r , the line is produced at. The radii that given lines are produced at are known approximately from reverberation mapping, and the GKN self-shielding photoionization model also predicts relative radii that agree well with the observed radii for NGC 5548 and other objects. For an inflowing BLR we expect the net inflow velocity, $v \propto r^{-0.5}$. In Figure 5, we compare the relative radii,

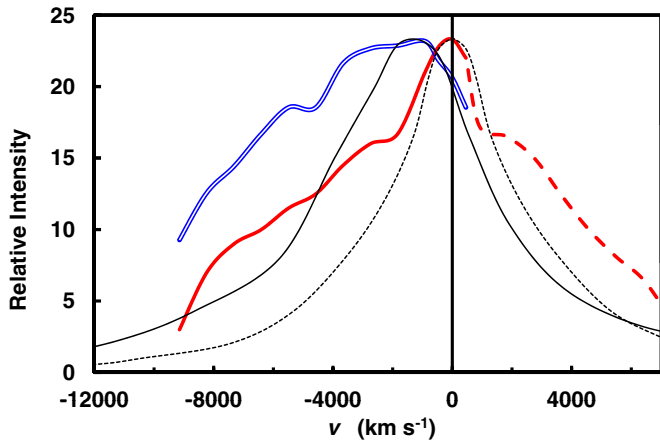


Figure 6. He II $\lambda 1640$ profiles estimated from composite profiles of SDSS AGNs with low blueshifting (red lines) and high blueshifting (double blue line). The C IV profiles for the same samples are shown as dotted and solid thin black lines, respectively. The red side of He II $\lambda 1640$ is heavily contaminated by O III] $\lambda 1640$ and is shown by the dashed red line. It is similar for both samples. The high-velocity blue wing of He II is dominated by C IV.

(A color version of this figure is available in the online journal.)

R , at which lines are emitted in the GKN model with the mean observed blueshifting velocities for AGNs. The mean blueshift velocity of C III] $\lambda 1909$ has been taken as half the blueshifting of C IV relative to Mg II (see Figure 3 of Corbin 1990), and other blueshift velocities have been taken from Tytler & Fan (1992). The predicted radii (in light days) are scaled to NGC 5548. While the blueshifts are for the large samples of AGNs studied by Corbin (1990) and Tytler & Fan (1992) rather than for NGC 5548 itself, there is a similar correlation if the mean blueshifts are plotted against the measured lags for NGC 5548. The least-squares fit line in Figure 5 gives $v \propto R^{-0.52}$ which is consistent with the expected slope of -0.50 .

The SDSS sample of Richards et al. (2002) provides additional support for increasing blueshifting with ionization. Figure 6 shows the He II $\lambda 1640$ and C IV $\lambda 1549$ blueshifts which we have derived from the composite SDSS profiles. It can be seen that for the sample with the highest blueshifts, the He II $\lambda 1640$ blueshift is approximately twice that of the C IV $\lambda 1549$ line as is predicted from the GKN model.

5. IMPLICATIONS

5.1. Mass Inflow Rate

It has long been noted that for pure radial motion, the mass transfer rate across the BLR is comparable to the accretion rate. Padovani & Rafanelli (1988) have argued, for example, that if the BLR is purely inflowing, then the mass inflow rate in AGNs correlates well with the accretion rate. Calculating the mass inflow rate is straight forward. We illustrate this by considering the C IV emitting region of the well-studied AGN NGC 5548. The sizes of the emitting regions are known in NGC 5548 from reverberation mapping and the continuum shape is also relatively well known. After reddening correction (Gaskell et al. 2004; Gaskell & Benker 2007), GKN get a bolometric luminosity of $10^{45.07}$ erg s^{-1} during the high state of NGC 5548 observed by Korista et al. (1995). (This is only slightly greater than the $10^{44.85}$ erg s^{-1} estimated by Padovani & Rafanelli 1988.) Using the GKN continuum, an observed C IV-emitting radius of 8 lt-day, and an electron density $n_H = 10^{10}$ cm^{-3} , CLOUDY photoionization models give a thickness

of $10^{13.7}$ cm for the C IV emitting region, and a mass of 1 solar mass. For an inflow velocity of 1000 km s^{-1} the inflow time from 8 lt-day is ~ 6 years. Adopting a 50% covering factor (see GKN), this gives a mass inflow rate of 0.08 solar masses per year.

If we adopt a black hole mass of $10^{7.9}$ solar masses from the average of the many NGC 5548 black hole mass estimates given by Vestergaard & Peterson (2006), and assume a standard radiative efficiency of 10%, then the Eddington accretion rate is 0.8 solar masses per year, and the accretion rate during the high state studied by GKN is 0.1 solar masses per year. This is comparable to the accretion rate we have calculated from the C IV emitting gas, so we can see that the BLR mass inflow can readily provide the mass inflow rate needed to power NGC 5548. Since the size of the C IV emitting region is well known from reverberation mapping and we know the covering factor to $\pm 50\%$, the main uncertainty in this calculation is the mean density. If the inflow velocities are less than hundreds of km s^{-1} , then one requires mean densities of the inflowing material of 10^{12} cm^{-3} or more.

Although we have calculated the mass inflow rate just for NGC 5548, it should be noted that there is no reason to think that NGC 5548 is unusual in this regard. Padovani & Rafanelli (1988) have shown that their estimated mass flow rates (calculated assuming that the entire BLR is moving radially) are proportional to the accretion rate needed to produce the bolometric luminosity for a wide variety of AGNs, including objects such as I Zw 1, which we now recognize as a high-accretion-rate narrow-line Seyfert 1.

5.2. Producing Inflow

Because of the degeneracy with the optical depth, the inflow velocity is not well constrained. However, the inflow velocity needed to explain the blueshifting is likely to be higher than the sound speed at the radius of the BLR. Is it possible to obtain such a net inflow velocity? In the classic Bondi solution, there is no problem in having supersonic infall at large distances, but this is unlikely to be relevant to what we are considering since the accreted material has angular momentum.

As is well known, to get a net inflow of matter there must be outward transport of angular momentum. This means that something must apply a torque on the gas. This could be magnetic breaking caused by a wind (Blandford & Payne 1982) or a viscosity providing a torque between material at different radii. The nature of the viscosity was a long-standing problem for accretion disk modeling, since ordinary gas viscosity is far too low, but it is now recognized that the necessary viscosity comes from the magneto-rotational instability (MRI; Balbus & Hawley 1991).

If we have inflow in the BLR, there is the same need for a torque to provide the necessary angular momentum transfer in the BLR gas. It would be natural for this to be provided by the same mechanisms as for the disk, i.e., magnetic breaking by a wind, or the MRI.

Visual inspection of magnetohydrodynamic (MHD) simulations of AGN accretion suggests that the turbulent and inflow velocities are roughly of the same magnitude, which is in qualitative agreement with our estimate of the inflow velocity. However, while there can be highly supersonic inflow in the “plunging region” (a few Schwarzschild radii from the black hole), the turbulent and inflow velocities in typical MHD simulations of rotationally supported Keplerian disks are subsonic at the radius of the BLR. There are however some simulations of gas with sub-Keplerian rotation with substantial inflow

velocities. One example is Proga & Begelman (2003) where the inflow velocity in the outer part of the simulations is $\sim 10\%$ of the Keplerian velocity (see the upper right panels in their Figures 9 and 10). Another possibility (Giri & Chakrabarti 2013) is that there is a two-component advective flow where a Keplerian disk is surrounded by a rapidly infalling sub-Keplerian halo.

Flares due to the tidal disruption of stars are a valuable laboratory for testing models of accretion disks because they arise from a well-defined injection of mass (~ 1 solar mass) in a one-off event. Cannizzo et al. (1990) used a time-dependent alpha-disk model to study the subsequent evolution of the accretion disk created. They concluded that the disk remained luminous for several thousand years. However, more recent work by Montesinos Armijo & de Freitas Pacheco (2011) shows that the duration of the flare (and disk) is of the order of only a few years to a few decades. This much shorter lifetime means that the inflow velocity is a couple of orders of magnitude higher than in the Cannizzo et al. (1990) model. Now that a number of tidal disruption events have been observed, we know that the duration is as in the Montesinos Armijo & de Freitas Pacheco (2011) models and hence that the inflow velocities are higher than in earlier models.

Although there is theoretical and observational support for relatively rapid (supersonic) inflow, more modeling of the motions around supermassive black holes is clearly needed.

5.3. The Relationship between the BLR and the Accretion Disk

It is now recognized that we are viewing most type 1 AGNs within $\sim 45^\circ$ of the axis (see Antonucci 1993 for a review), and hence that we view the BLR close to face on. Even when we see disk-like line profiles, the inclinations are still not great (see, for example, Eracleous & Halpern 1994 and Figure 2 of Gaskell 2011). Because the observed broad-line widths are substantial, and the BLR has to be flattened (see GKN), there *must* be a *substantial* component of random BLR velocity out of the plane (Gaskell 2009). Such a velocity is also necessary to maintain the thickness of the BLR needed to provide the observed covering factor.

The overall motion of the BLR (see Gaskell 2009) has to be as follows: the main motion is rotational but there is a vertical random (“turbulent”) component of velocity (Osterbrock 1978) that is almost as great as the rotational velocity. Then, as argued above, there is an additional slower net inflow. As we have noted, this overall structure of the velocity field in the BLR is qualitatively similar to the results of accretion disk MHD calculations (see, for example, the simulations of Hawley & Krolik 2001). Gaskell (2008) points out that the size of the accretion disk is such that its outer parts (those generating the optical and IR emission) must extend out to within the BLR. We therefore propose on the basis of the similarities of the size, physical processes needed, kinematics, and mass inflow rates, that *the BLR and the outer part of the accretion disk are one and the same*. The accretion disk is the part which is optically thick in the continuum and closest to the equatorial plane.

The magnetic fields generated by the MRI potentially solve two major problems. The first is the long-standing “confinement problem” (see Mathews & Capriotti 1985 for a review). Rees (1987) has shown how magnetic fields can confine the BLR clouds. A second problem is the survival problem. Clouds with a random velocity component (e.g., as proposed by Osterbrock 1978) have a mean time between collisions comparable to the orbital timescale (see Osterbrock & Mathews 1986). Cloud–cloud

collisions will produce very high Mach number shocks which will immediately destroy the colliding clouds. Strong magnetic fields can prevent shocks from occurring, just as they prevent such shocks in MHD simulations of accretion disks.

6. DISCUSSION

6.1. High-accretion-rate AGNs

As discussed in the Introduction, it is well established that high-accretion-rate AGNs (such as NLS1s) show strong blueshifting, and this has been interpreted as evidence for strong outflowing winds in high-accretion-rate AGNs (e.g., Leighly & Moore 2004; Komossa et al. 2008). However, the blueshiftings in NLS1s are merely the extreme of the distribution for AGNs in general, so there is no reason to think that they have a different cause from the shifts in other AGNs. We therefore propose that the greater blueshifts in NLS1 imply greater *inflow* rates. This result follows quite naturally from our *STOKES* modeling shown in Figure 1. The amplitude of the blueshifting obviously depends linearly on the inflow velocity, but as shown in Figure 1, it also depends on the optical depth and covering factor. An inflow velocity of 1000 km s^{-1} , as we have assumed above, is adequate to explain the typical blueshiftings, but for the most extreme examples, such as Q1338+416, where the shift is almost 5000 km s^{-1} (Corbin 1990), a higher inflow velocity is needed. In Figure 1, the blueshifting is roughly proportional to the product of the scattering optical depth and the inflow velocity. For a given column length the optical depth depends on the filling factor and density. The mass inflow rate is proportional to the mean density and inflow rate. Thus, whether a greater optical depth or a greater inflow velocity is responsible for the increased blueshifts, *the blueshift is proportional to the mass inflow rate*.

6.2. Estimating Black Hole Masses from C IV Widths

There is considerable interest in estimating the masses of black holes at high redshifts. Because it is difficult to measure $H\beta$ at high redshift, it has been suggested that the FWHM of C IV $\lambda 1549$ can be used instead of the FWHM of $H\beta$ (Vestergaard 2002; Warner et al. 2003). Our conclusion that the C IV-producing region has a net inflow rather than an outflow in a wind is good news for such endeavors. However, the FWHM of C IV needs to be used with caution because, not only does scattering cause blueshifting, but it also *broadens* the lines (see Figure 1). The width of C IV can therefore give an overestimate of the virial velocity in the C IV emitting region. Since it is the square of the line width which enters into the equation for the virial mass, significant systematic errors in the black hole mass can be introduced. We have noted above that the blueshifting increases with accretion rate, and that it has also been found to be correlated with radio loudness and the presence of broad absorption lines, so there is a danger of systematic errors when using the FWHM of C IV to estimate masses. It should, however, be possible to empirically correct for these systematic errors by investigating the differences in masses estimated from high- and low-ionization lines as a function of the blueshifting.

6.3. Blueshifts of Narrow Lines

It has long been known (Burbidge et al. 1959) that *narrow* lines in AGNs are blueshifted, and it has been widely assumed that this is a consequence of outflow of the NLR gas and dust (e.g., Dahari & De Robertis 1988). Zamanov et al. (2002) showed that the blueshifting of [O III] $\lambda 5007$ is correlated with

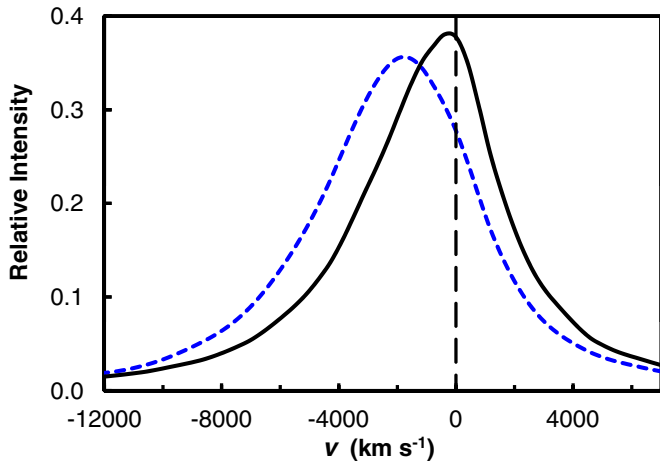


Figure 7. Theoretical C IV line profiles for electron or Rayleigh scattering off a inflowing flared disk of half-opening angle 60° , an inflow velocity of 1000 km s^{-1} , and a radial optical depth of 5. The solid black curve shows the profile predicted when the system is viewed away from the disk. The dashed blue line shows the profile predicted when the system is viewed from just inside the disk surface as could be the case in a BALQSO.

(A color version of this figure is available in the online journal.)

the blueshifting of a broad C IV line and that both blueshiftings are strongest in NLS1s. This is confirmed by Komossa et al. (2008) who have also shown that the blueshiftings of the narrow lines increase with ionization potential. Corbin (1990, 1992) found that the blueshiftings of C IV were related to the C IV Baldwin effect (Baldwin 1977; Baldwin et al. 1978). This is also very obvious in Figure 4 of Richards et al. (2002). Zhang et al. (2011) show that the O [III] blueshiftings are similarly related to the O [III] Baldwin effect. The NLR blueshiftings thus show many striking similarities to the BLR blueshiftings. Zamanov et al. (2002) argue that the correlation of blueshiftings points to a kinematic connection between the BLR and NLR. We therefore suggest that if the BLR blueshiftings are due to inflow and scattering, then so too are the NLR blueshiftings.

6.4. Broad Absorption Line QSOs and Orientation Effects

Corbin (1990) discovered that his sample of BALQSOs showed unusually large blueshiftings of C IV with respect to Mg II ($\sim 1700 \text{ km s}^{-1}$). Furthermore, he found that the BALQSOs also deviated from the correlation between blueshifting and the Baldwin effect found for non-BALQSOs. This is in the sense that their blueshifts are too large for their equivalent widths. This suggests that there is some additional factor influencing the blueshifting. Since BALQSOs are believed to be seen at higher inclinations (Hines & Wills 1995; Goodrich & Miller 1995; Cohen et al. 1995; Elvis 2000), orientation could be the factor enhancing or even causing the blueshifting of high-ionization lines in BALQSOs (Richards et al. 2002). Our STOKES simulations verify that in our scattering+inflow model there is indeed an enhancement of the blueshifting at high inclinations. We find a negligible dependence of the blueshifting on viewing angle within the half-opening angle of the torus (i.e., from any type ~ 1 viewing position), but that there is a strong increase of the blueshifting as we start seeing through the scattering medium (see Figure 7). The increase in blueshift is because the scattered light becomes more important. In our models, this is a relatively abrupt transition (i.e., from all type 1 viewing positions the predicted line profile is like the solid black line in Figure 7, while for all lines of sight passing through the

scattering disk the profiles are like the blue dashed line). In a real AGN the material will be clumpy and the transition will probably not be as abrupt.

For the models shown in this paper we have used an unchanging unscattered profile, but since observations strongly point to the BLR being flattened and rotating (see Introduction) the unscattered profile will actually be broader when seen at higher inclinations. Our model thus also predicts that when high-ionization lines are highly blueshifted because the inclination is higher, there will be further broadening in addition to that caused by the scattering. Inspection of Table 2 of Richards et al. (2002) shows that the more blueshifted C IV lines are indeed broader.

Note that we do *not* predict that a large blueshift will be observed in type 2 AGNs. This is because the central region is by definition obscured by the torus and if the BLR is detectable in polarized light, then the scatterers sending light into our line of sight are located far from the central region.

6.5. Determining the Structure of the Scattering Region(s)

The ease with which scattering off inflowing material with differing geometries reproduces the observed blueshifting provides gratifying support for our inwardly spiraling BLR picture. However, a disappointment is that the blueshifting is insensitive to the geometry (see Figures 1 and 2), and because there is some degeneracy between the inflow rate, covering factor, and optical depth, we cannot get a strong constraint on the geometry and kinematics because of the limited accuracy with which line profiles can be measured. Fortunately, other observations provide constraints on the geometry and kinematics. Two promising ways of studying the distribution and kinematics of the scatters are spectropolarimetry (e.g., Smith et al. 2004, 2005; Goosmann & Gaskell 2007; Marin et al. 2012) and polarimetric reverberation mapping (Gaskell et al. 2012). The combination of the two methods (i.e., high-resolution spectropolarimetric reverberation mapping) promises to be particularly powerful.

7. CONCLUSIONS

We have pointed out the problems with the popular outflow/wind explanation (Gaskell 1982) for the blueshifting and blueward asymmetry of the high-ionization lines, and shown that velocity-resolved reverberation mapping supports the velocity field of the BLR having an inflow velocity component. We have demonstrated using the STOKES Monte Carlo radiative transfer code that electron or Rayleigh scattering off an inflowing medium readily reproduces the blueshifts and asymmetries of the high-ionization lines. Our model also predicts that the relative blueshifts for different lines in the same AGN should be proportional to the inverse-square root of the radius the lines are expected to be formed at. Available estimates of relative blueshiftings support this.

If the BLR is indeed inwardly spiraling, then this has many important implications. Viscosity is required to transport angular momentum outward. As with traditional accretion disks, this is presumably due to the MRI. As the BLR inflows it releases energy. The deduced mass inflow rates are comparable to the mass accretion rate needed to power AGNs. We have therefore proposed that the BLR could be a major part of the material accreting onto the black hole. Taken together, these conclusions suggest a picture where *the BLR is part of the outer region of the accretion disk*.

We have argued that the magnitude of the high-ionization blueshifting effect is proportional to the mass-inflow rate. The inflowing BLR picture thus naturally explains why high-accretion-rate AGNs (NLS1s) show the largest high-ionization-line blueshifts. Our models also gives an explanation of why BALQSOs can show higher blueshifts if they are seen at higher inclinations.

The inwardly spiraling BLR picture supports the use of C IV to measure black hole masses in high-redshift AGNs but, because scattering broadens lines as well as blueshifting them, caution is necessary when using C IV line widths. A systematic correction could be necessary as a function of the blueshifting.

Similarities between NLR and BLR blueshiftings suggest that NLR blueshiftings might also be due to an inflow velocity component and scattering.

Finally, as Korista & Ferland (1998) have pointed out, Rayleigh scattering could be important in AGNs in the ultra-violet, and we have proposed a simple observational test for the degree to which Rayleigh scattering influences the blueshifting.

R.G. is grateful to the Astronomy Department of the University of Texas for its hospitality during his time as a Tinsley scholar where this work was begun. We would like to thank Philip Hardee, Liz Klimek, Julian Krolik, Bill Mathews, Matias Montesinos, Ramesh Narayan, Daniel Proga, and Greg Shields for helpful discussions of various issues. This research has been supported in part by the US National Science Foundation through grants AST 03-07912 and AST 08-03883, by the Space Telescope Science Institute through grant AR-09926.01, the GEMINI-CONICYT Fund of Chile through project No. 32070017, FONDECYT of Chile through project No. 1120957, French grant ANR-11-JS56-013-01, the French *GdR* PCHE, and from the Center for Theoretical Astrophysics (CTA) through Czech Ministry of Education, Youth and Sports program LC06014. Finally, we would like to thank the anonymous referee for helpful comments.

REFERENCES

- Antonucci, R. R. J. 1993, *ARA&A*, 31, 473
 Antonucci, R. R. J. 2012, *A&AT*, 27, 557
 Auer, L. H., & van Blerkom, D. 1972, *ApJ*, 178, 175
 Balbus, S. A., & Hawley, J. F. 1991, *ApJ*, 376, 214
 Baldwin, J. A. 1975, *ApJ*, 201, 26
 Baldwin, J. A. 1977, *ApJ*, 214, 679
 Baldwin, J. A., Burke, W. L., Gaskell, C. M., & Wampler, E. J. 1978, *Natur*, 273, 431
 Blandford, R. D., & McKee, C. F. 1982, *ApJ*, 255, 419
 Blandford, R. D., & Payne, D. G. 1982, *MNRAS*, 199, 883
 Blumenthal, G. R., & Mathews, W. G. 1975, *ApJ*, 198, 517
 Brotherton, M. S., Wills, B. J., Francis, P. J., & Steidel, C. C. 1994, *ApJ*, 430, 495
 Burbidge, E. M., Burbidge, G. R., & Prendergast, K. H. 1959, *ApJ*, 130, 26
 Cannizzo, J. K., Lee, H. M., & Goodman, J. 1990, *ApJ*, 351, 38
 Cherepashchuk, A. M., & Lyutyi, V. M. 1973, *ApL*, 13, 165
 Clavel, J., Reichert, G. A., Alloin, D., et al. 1991, *ApJ*, 366, 64
 Cohen, M. H., Ogle, P. M., Tran, H. D., et al. 1995, *ApJL*, 448, L77
 Collin-Souffrin, S., Dyson, J. E., McDowell, J. C., & Perry, J. J. 1988, *MNRAS*, 232, 539
 Corbin, M. R. 1990, *ApJ*, 357, 346
 Corbin, M. R. 1992, *ApJ*, 391, 577
 Crenshaw, D. M., & Blackwell, J. H., Jr. 1990, *ApJL*, 358, L37
 Dahari, O., & De Robertis, M. M. 1988, *ApJ*, 331, 727
 Denney, K. D., Peterson, B. M., Pogge, R. W., et al. 2009, *ApJL*, 704, L80
 Done, C., & Krolik, J. H. 1996, *ApJ*, 463, 144
 Elvis, M. 2000, *ApJ*, 545, 63
 Eracleous, M., & Halpern, J. P. 1994, *ApJS*, 90, 1
 Ferland, G. J., Korista, K. T., Verner, D. A., et al. 1998, *PASP*, 110, 761
 Ferrara, A., & Pietrini, P. 1993, *ApJ*, 405, 130
 Gaskell, C. M. 1982, *ApJ*, 263, 79
 Gaskell, C. M. 1983, in Proc. Liege Intl. Astrophys. Colloq. 24, Quasars and Gravitational Lenses, 473
 Gaskell, C. M. 1988, *ApJ*, 325, 114
 Gaskell, C. M. 1996, *ApJL*, 464, L107
 Gaskell, C. M. 2008, *RMxAA*, 32, 1
 Gaskell, C. M. 2009, *NewAR*, 53, 140
 Gaskell, C. M. 2010a, *Natur*, 463, E1
 Gaskell, C. M. 2010b, in ASP Conf. Ser. 427, Accretion and Ejection in AGN: A Global View, ed. L. Maraschi, G. Ghisellini, R. Della Ceca, & F. Tavecchio (San Francisco, CA: ASP), 68
 Gaskell, C. M. 2010c, *ApJ*, submitted (arXiv:1008.1057)
 Gaskell, C. M. 2011, *BaltA*, 20, 392
 Gaskell, C. M., & Benker, A. J. 2007, *ApJ*, submitted (arXiv:0711.1013)
 Gaskell, C. M., Brandt, W. N., Dietrich, M., Dultzin-Hacyan, D., & Eracleous, M. 1999, in ASP Conf. Ser. 175, Structure and Kinematics of Quasar Broad Line Regions, ed. C. M. Gaskell, W. N. Brandt, M. Dietrich, D. Dultzin-Hacyan, & M. Eracleous (San Francisco, CA: ASP)
 Gaskell, C. M., Goosmann, R. W., Antonucci, R. R. J., & Whysong, D. H. 2004, *ApJ*, 616, 147
 Gaskell, C. M., Goosmann, R. W., Merkulova, N. I., Shakhovskoy, N. M., & Shoji, M. 2012, *ApJ*, 749, 148
 Gaskell, C. M., Klimek, E. S., & Nazarova, L. S. 2007, *ApJ*, submitted (arXiv:0711.1025) (GKN)
 Gaskell, C. M., & Snedden, S. A. 1997, *BAAS*, 29, 1252
 Gaskell, C. M., & Snedden, S. A. 1999, in ASP Conf. Ser. 175, Structure and Kinematics of Quasar Broad Line Regions, ed. C. M. Gaskell, W. N. Brandt, M. Dietrich, D. Dultzin-Hacyan, & M. Eracleous (San Francisco, CA: ASP), 157
 Gaskell, C. M., & Sparke, L. S. 1986, *ApJ*, 305, 175
 Giri, K., & Chakrabarti, S. K. 2013, *MNRAS*, 430, 2836
 Goodrich, R. W., & Miller, J. S. 1995, *ApJL*, 448, L73
 Goosmann, R. W., & Gaskell, C. M. 2007, *A&A*, 465, 129
 Goosmann, R. W., Mouchet, M., Czerny, B., et al. 2007, *A&A*, 475, 155
 Hawley, J. F., & Krolik, J. H. 2001, *ApJ*, 548, 348
 Hines, D. C., & Wills, B. J. 1995, *ApJL*, 448, L69
 Kallman, T. R., & Krolik, J. H. 1986, *ApJ*, 308, 805
 Kallman, T. R., Wilkes, B. J., Krolik, J. H., & Green, R. 1993, *ApJ*, 403, 45
 Kaneko, N., & Ohtani, H. 1968, *AJ*, 73, 899
 Kollatschny, W. 2003, *A&A*, 407, 461
 Kollatschny, W., & Dietrich, M. 1996, *A&A*, 314, 43
 Komossa, S., Xu, D., Zhou, H., Storchi-Bergmann, T., & Binette, L. 2008, *ApJ*, 680, 926
 Koratkar, A. P., & Gaskell, C. M. 1989, *ApJ*, 345, 637
 Koratkar, A. P., & Gaskell, C. M. 1991a, *ApJ*, 375, 85
 Koratkar, A. P., & Gaskell, C. M. 1991b, *ApJS*, 75, 719
 Korista, K. T., Alloin, D., Barr, P., et al. 1995, *ApJS*, 97, 285
 Korista, K. T., & Ferland, G. J. 1998, *ApJ*, 495, 672
 Krolik, J. H., Horne, K., Kallman, T. R., et al. 1991, *ApJ*, 371, 541
 Laor, A. 2006, *ApJ*, 643, 112
 Lee, H.-W. 2005, in ASP Conf. Ser. 343, Astronomical Polarimetry: Current Status and Future Directions, ed. A. Adamson, C. Aspin, C. J. Davis, & T. Fujiyoshi (San Francisco, CA: ASP), 441
 Leighly, K. M., & Moore, J. R. 2004, *ApJ*, 611, 107
 Lynds, C. R. 1967, *ApJ*, 147, 396
 Lyutyi, V. M., & Cherepashchuk, A. M. 1972, *ATsir*, 688, 1
 Marin, F., Goosmann, R. W., Gaskell, C. M., Porquet, D., & Dovčiak, M. 2012, *A&A*, 548, A121
 Marziani, P., & Sulentic, J. W. 2012, *NewAR*, 56, 49
 Mathews, W. G., & Capriotti, E. R. 1985, in Astrophysics of Active Galaxies and Quasi-Stellar Objects, ed. J. S. Miller (Mill Valley, CA: Univ. Science Books), 185
 Mathews, W. G. 1993, *ApJL*, 412, L17
 Mathis, J. S. 1970, *ApJ*, 162, 761
 Montesinos Armijo, M., & de Freitas Pacheco, J. A. 2011, *ApJ*, 736, 126
 Onken, C. A., & Peterson, B. M. 2002, *ApJ*, 572, 746
 Osterbrock, D. E. 1978, *PNAS*, 75, 540
 Osterbrock, D. E. 1993, *ApJ*, 404, 551
 Osterbrock, D. E., & Mathews, W. G. 1986, *ARA&A*, 24, 171
 Padovani, P., & Rafanelli, P. 1988, *A&A*, 205, 53
 Paltani, S., & Türler, M. 2003, *ApJ*, 583, 659
 Peterson, B. M., & Wandel, A. 2000, *ApJL*, 540, L13
 Popović, L. Č. 2012, *NewAR*, 56, 74
 Pounds, K. A., Nandra, K., Stewart, G. C., George, I. M., & Fabian, A. C. 1990, *Natur*, 344, 132
 Proga, D., & Begelman, M. C. 2003, *ApJ*, 592, 767

- Pronik, V. I., & Sergeev, S. G. 2006, in ASP Conf. Ser. 360, AGN Variability from X-Rays to Radio Waves, ed. C. M. Gaskell, I. M. McHardy, B. M. Peterson, & S. G. Sergeev (San Francisco, CA: ASP), 13
- Rees, M. J. 1987, *MNRAS*, **228**, 47P
- Richards, G. T., Vanden Berk, D. E., Reichard, T. A., et al. 2002, *AJ*, **124**, 1
- Risaliti, G., Maiolino, R., & Salvati, M. 1999, *ApJ*, **522**, 157
- Rokaki, E., Lawrence, A., Economou, F., & Mastichiadis, A. 2003, *MNRAS*, **340**, 1298
- Sergeev, S. G., Pronik, V. I., Peterson, B. M., Sergeeva, E. A., & Zheng, W. 2002, *ApJ*, **576**, 660
- Shields, G. A., & McKee, C. F. 1981, *ApJL*, **246**, L57
- Smith, J. E., Robinson, A., Alexander, D. M., et al. 2004, *MNRAS*, **350**, 140
- Smith, J. E., Robinson, A., Young, S., Axon, D. J., & Corbett, E. A. 2005, *MNRAS*, **359**, 846
- Snedden, S. A., & Gaskell, C. M. 2004, in ASP Conf. Ser. 311, AGN Physics with the Sloan Digital Sky Survey, ed. G. T. Richards & P. B. Hall (San Francisco, CA: ASP), 197
- Snedden, S. A., & Gaskell, C. M. 2007, *ApJ*, **669**, 126
- Steidel, C. C., & Sargent, W. L. W. 1991, *ApJ*, **382**, 433
- Sulentic, J. W., Marziani, P., & Dultzin-Hacyan, D. 2000, *ARA&A*, **38**, 521
- Sulentic, J. W., Marziani, P., Dultzin-Hacyan, D., Calvani, M., & Moles, M. 1995, *ApJL*, **445**, L85
- Sulentic, J. W., Zwitter, T., Marziani, P., & Dultzin-Hacyan, D. 2000, *ApJL*, **536**, L5
- Tytler, D., & Fan, X.-M. 1992, *ApJS*, **79**, 1
- Vestergaard, M. 2002, *ApJ*, **571**, 733
- Vestergaard, M., & Peterson, B. M. 2006, *ApJ*, **641**, 689
- Warner, C., Hamann, F., & Dietrich, M. 2003, *ApJ*, **596**, 72
- Welsh, W. F., Martino, D. L., Kawaguchi, G., & Kollatschny, W. 2007, in ASP Conf. Ser. 373, The Central Engine of Active Galactic Nuclei, ed. L. C. Ho & J.-M. Wang (San Francisco, CA: ASP), 29
- Weymann, R. J. 1970, *ApJ*, **160**, 31
- Wilkes, B. J. 1984, *MNRAS*, **207**, 73
- Wilkes, B. J., & Carswell, R. F. 1982, *MNRAS*, **201**, 645
- Wills, B. J., & Browne, I. W. A. 1986, *ApJ*, **302**, 56
- Xu, D. W., Komossa, S., Wei, J. Y., Qian, Y., & Zheng, X. Z. 2003, *ApJ*, **590**, 73
- Zamanov, R., Marziani, P., Sulentic, J. W., et al. 2002, *ApJL*, **576**, L9
- Zhang, K., Dong, X.-B., Wang, T.-G., & Gaskell, C. M. 2011, *ApJ*, **737**, 71